Computers and Electrical Engineering 69 (2018) 129–141

Contents lists available at ScienceDirect

Computers and Electrical Engineering

journal homepage: www.elsevier.com/locate/compeleceng

Data mining-based high impedance fault detection using mathematical morphology☆

Kavaskar Sekar[a,*], Nalin Kant Mohanty[b]

[a] Department of Electrical and Electronics Engineering, Panimalar Engineering College, Anna University, Chennai, Tamil Nadu 600123, India
[b] Department of Electrical and Electronics Engineering, Sri Venkateswara College of Engineering, Sriperumbudur, Tamil Nadu 602 117, India

ARTICLE INFO

Keywords:
High impedance fault
Distribution system
Mathematical morphology
Decision tree
Data mining

ABSTRACT

High impedance fault (HIF) detection is a challenging task in power system protection because of the random nature of current. HIFs are not efficiently detected by conventional protection systems because of their low current magnitudes. The proposed method presents an intelligent HIF protection technique using Mathematical Morphology (MM) and a data mining-based Decision Tree (DT) model. The current signals are produced by a MATLAB / SIMULINK model of an actual distribution system with real data. The features of these current signals are computed after processing with MM filter. A data mining-based DT model is then generated using these features of the current signals, and this DT model makes a final decision on classification into HIF and non-HIF. The proposed scheme is tested on different HIF and non-HIF cases and the results were found to be encouraging.

1. Introduction

In distribution systems, High Impedance Faults (HIFs) occur due to downed live conductors connected to a high impedance ground surface or unbroken conductor touching leaning tree. This contact restricts the current value between 0 and 75 A depending on the high impedance surface [1]. The conventional relays are incapable of detecting currents with these low magnitudes. In this context, fallen live conductors pose a threat to humans and their property. HIFs in distribution systems often generate fires and cause loss of power supply to consumers. Therefore, HIF detection has now become a big issue for power utilities. In this work, a 11 kV system is chosen because a huge number of HIFs come with supply voltages of 15 kV or less, with the difficulty faced in HIF detection being worse at lower voltages. The difficulty is less severe above 15 kV, but HIFs can occur at these voltages as well [1].

The HIF phenomena and detection methods are comprehensively documented in [2]. The method proposed in [3] measures and analyzes the harmonic content to understand what extent this is useful in HIF detection. Another method based on the concept of fractal geometry analyzes chaotic properties of fault current [4]. The primary problem with these methods is setting a threshold, which affects the performance of the detection method.

A reliable detection scheme using time-frequency analysis for feature extraction is in [5,6]. Time-frequency analysis is highly sensitive to a non-stationary signal and shows good performance in all the detection criteria. However, the time consumed during the computations raises a question about the utilization of this method in protection applications.

The Wavelet Transform (WT) method is capable of processing the signal by analyzing low- and high-frequency components. A method based on WT detects HIF using wavelet decomposed coefficient of a voltage signal [7,8]. Both voltage and current signal

☆ Reviews processed and recommended for publication to the Editor-in-Chief by Guest Editor Dr. B.V.

* Corresponding author.
E-mail address: kavaskarsekar@gmail.com (K. Sekar).

https://doi.org/10.1016/j.compeleceng.2018.05.010
Received 19 April 2017; Received in revised form 8 May 2018; Accepted 9 May 2018

Fig. 1. The Proposed HIF detection method.

features are extracted using wavelet packet transform for detection and discrimination of HIF [9]. The standard deviation of detail and approximation coefficient of level 3 [10] and level 7 [11] of db4 mother wavelet is used for the detection process. In addition to WT feature extraction, Principal Component Analysis (PCA), Bayes classifier [12,13] and fuzzy inference system [14] are used for classification into HIF and non-HIF. WT provides a better resolution in signal processing. However, high computational burden, high sampling rate and memory space requirements restrict the use of this method in protection applications. In [15], the amplitude and phase information of HIF current signal is proposed. Mathematical Morphology (MM) [16,17] was recently employed in HIF detection and the method needs an enhancement.

From these prior detection methods significant properties of HIFs are observed. However, detection delay has not been reported except in [4,13,16,17]. Moreover, majority of detection methods have chosen a high sampling rate while observing the input signal for processing. High sampling rate increases the computational work and memory space requirements. Hence, this paper proposes a superior method with low sampling rate and exceptional speed in processing the signal which reduces both computational work and memory space requirements.

In this paper, an enhanced method shown in Fig. 1 is proposed for HIF detection. The HIF and non-HIF current signal data are observed from an accurate MATLAB / SIMULINK model of an actual electric power distribution system. MM is a non-linear and time domain signal transformation tool. It uses simple calculations because of which processing time is reduced. Hence, MM filters are appropriate for real-time power system applications like transmission line protection. The advantages of MM have been established in many aspects [19,20]. In the signal processing method, the most important task of MM operators is to extract significant features and this is done by the interaction between the signal and Structured Element (SE). SE shape is a key factor in signal processing. The MM filter is used for the pre-processing of the current signal in this work. This filter reduces the noise in the signal and at the same time preserves features of fault current. The features of the current signal are then used to generate a data mining-based decision tree model that differentiates HIF from non-HIF power system disturbances.

The rest of this paper is organized as follows: Section 2 presents HIF characteristics. The system studied and the simulation cases are described in Sections 3 and 4 respectively. Section 5 provides a detailed performance analysis of the pre-processing filter. Different features of the current signal and data mining-based decision tree model for feature classification are presented in Sections 6 and 7 respectively. The simulation results are illustrated in Section 8 and discussion of the results is provided in Section 9. Finally, the conclusions are presented in Section 10.

2. HIF characteristics

The occurrence of HIF becomes a more severe problem if it is on distribution voltages that are less than 15 kV. HIFs are usually accompanied with an arc, and so, HIF current has significant properties such as asymmetry, non-linearity, build-up, intermittence, and shoulder [2,6,9].

1. Asymmetry: Peak values of the current for both positive and negative half cycles are dissimilar.
2. Non-linearity: The voltage and current characteristics are non-linear because of the presence of harmonics.
3. Intermittence: An energized wire that comes in contact with a tree branch separates due to wind force in a few cycles or downed conductor has poor interaction with the soil.
4. Build-up: The magnitude of current augments steadily from a low value to a steady-state value.
5. Shoulder: The increase in current pauses for a few cycles and then build-up.

To generate the current signal with the properties mentioned above, the new HIF model based on several Emanuel HIF arc models [9,18] is used as shown in Fig. 2. To illustrate, five different HIF current signals generated using the model are shown in Fig. 3. The arc parameter data for those signals are provided in Table 1. The *V–I* characteristics of the HIF model of state 4 is shown in Fig. 4. Note that the HIF signals have all properties mentioned above. Thus, the chosen model is used to represent HIF in the proposed detection method.

3. System studied

Since HIF data collection from the power utility system is not an easy task due to reliability and economic reasons, an actual electric power distribution system has been accurately modeled with real data using MATLAB / SIMULINK. A 11 kV electric power distribution system in Chennai (India) was chosen to study the system as shown in Fig. 5. The 11 kV bus is energized through a couple of distribution transformers with the rating of 33/11 kV, 16 MVA, and Delta-Star connection. The electric power distribution system with 7 distribution feeders comprises 4.2 km long underground cables and 21.8 km long overhead lines connected to 102 loads

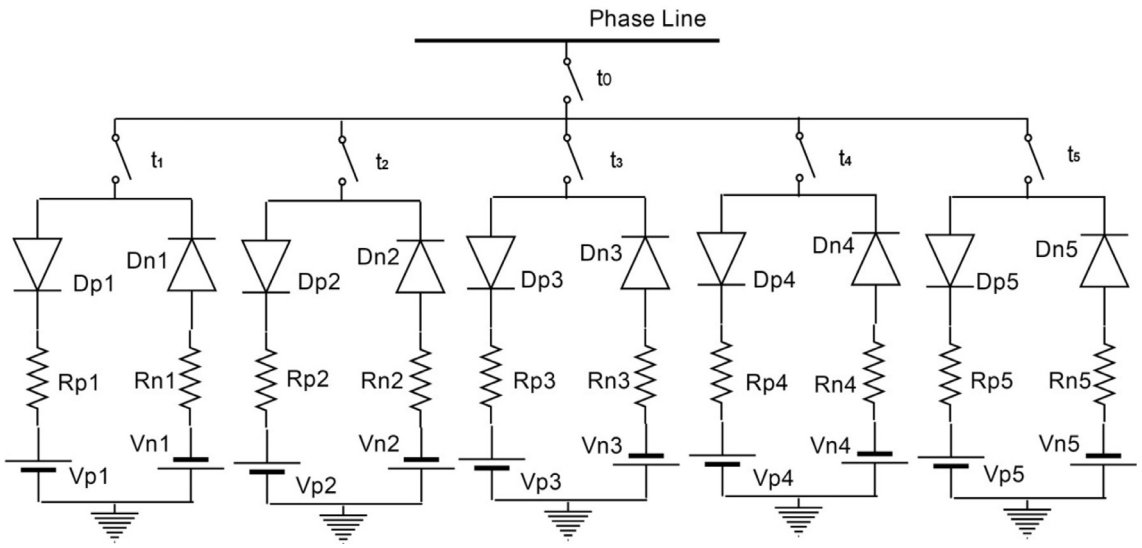

Fig. 2. HIF model.

including industrial loads. Table 2 presents the load data of the electric power distribution system.

4. Data collection

A MATLAB / SIMULINK model of the distribution system was used to collect the current signal for both HIF and non-HIF cases. By changing parameters like resistance and D.C voltage of the HIF model, different HIF currents in the range of 2–75 A were obtained. Load current waveforms were produced by connecting both linear (static and motor type of load) and non-linear loads. Different load switching current waveforms were generated by connecting non-linear to linear load ratio of 1–0.5 with different load switching instances.

The transformer current is in the saturation area of the excitation curve when the transformer is switched with no load. Moreover, this current is non-linear in nature and creates a high magnitude asymmetrical current. The transformer inrush currents involve a long-lasting DC component which is rich in harmonics. The nonlinearity, asymmetry, and harmonics in the current signal are the properties of magnetic inrush current which bear a close resemblance to HIF characteristics. Therefore, it is necessary to discriminate HIF from this inrush current to avoid incorrect operation in the protection system [6].

In this work, it is to be noted that the capacitor bank of 1 Mvar is connected with 11 kV bus. The current signals due to capacitance switching were simulated with different switching instances. Thus, from the above study 1000 test cases (540 HIF + 460 Non-HIF) were simulated with a sampling frequency of 3 kHz. Complete information about simulation study is presented in Table 3.

5. Pre-processing

MM is acquired from Set Theory and Integral Geometry, and it is an important tool in geometrical investigation. MM has been widely used as a signal processing technique and applied to power system problems [16,17]. MM is a non-linear technique which extracts information on high- and low-frequency signals [19,20]. Since MM uses simple arithmetic operations such as addition and subtraction, it has a lower processing time because of simpler calculations. It uses SE to extract significant and essential features of the signals. The shape of SE may be selected based on expected nature of the signal to be processed [19].

If f (x) is the input signal and g(y) is the SE, the two fundamental operations in MM called dilation and erosion can be defined as follows:

Dilation ($\oplus$) of the signal f(x) by g(y) is given in Eq. (1):

$$y_d(x) = (f \oplus g)(x) = \max\{f(x-y) + g(y)\},\ \ 0 \le (x-y) \le x,\ \ y \ge 0 \tag{1}$$

Erosion Θ of the signal f(x) by g(y) is given in Eq. (2):

$$y_e(x) = (f \ominus g)(x) = \min\{f(x+y) - g(y)\},\ \ 0 \le (x+y) \le 0,\ \ y \ge 0 \tag{2}$$

Further, these two primary functions are used to derive the opening and closing operations. Opening ($\bigcirc$) normally smoothens the sharp end, while closing ($\bullet$) fills up the narrow valleys of the signal. These operations are defined in Eqs. (3) and (4) as follows:

$$y_o(x) = (f \circ g)(x) = ((f \ominus g) \oplus g)(x) \tag{3}$$

$$y_c(x) = (f \bullet g)(x) = ((f \oplus g) \ominus g)(x) \tag{4}$$

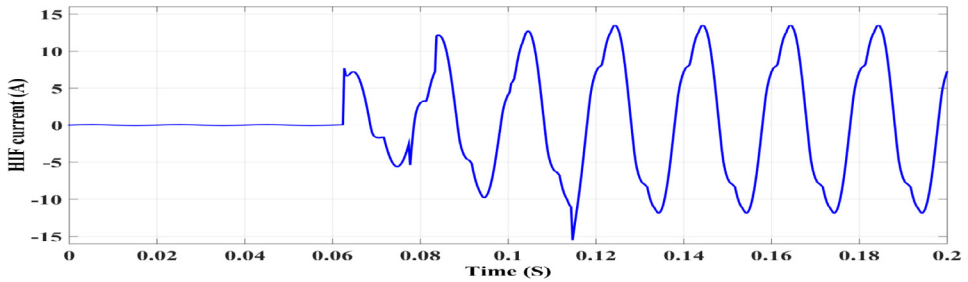

(a)

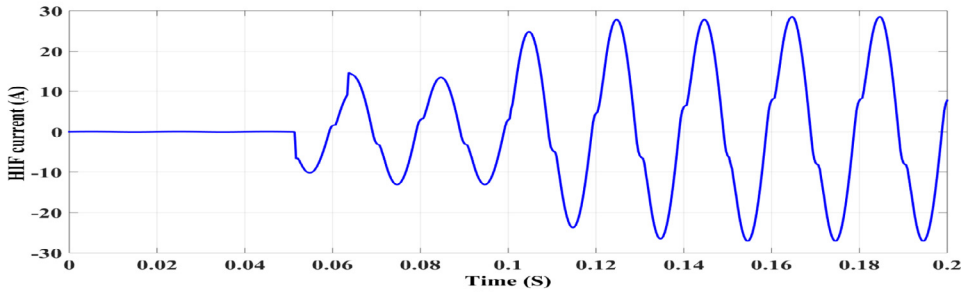

(b)

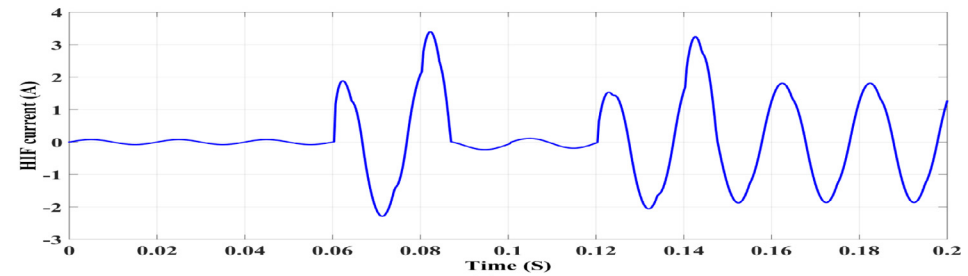

(c)

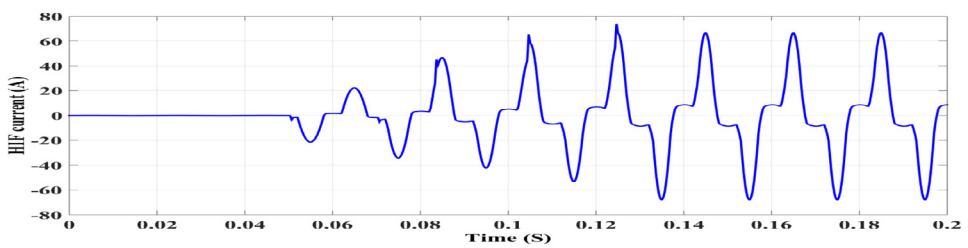

(d)

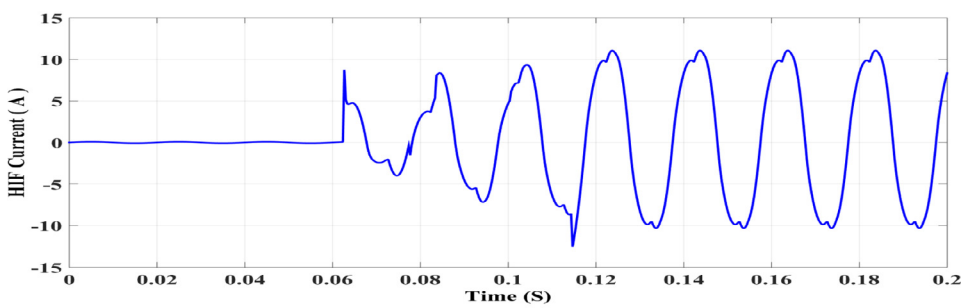

(e)

Fig. 3. Simulated HIF current of (a) State 1 (b) state 2 (c) state 3 (d) State 4 (e) State 5.

Table 1
Arc parameters for 5 different conditions.

State	Arc parameters	1	2	3	4	5
State 1	t (S)	0.0625[a]	0.076[a]	0.105[a]	0.116[a]	0.083[a]
$t_0 = 0$[a]	Rp (Ohms)	1200	2900	4550	3730	4010
	Rn (Ohms)	1000	3010	4000	3760	4020
	Vp (Volts)	4060	8020	7560	10,010	5000
	Vn (Volts)	4500	8100	7680	10,500	5200
State 2	t (S)	0.051[a]	0.063[a], 0.15[b]	0.12[a]	0.085[a]	0.108[a]
$t_0 = 0$[a]	Rp (Ohms)	550	2800	2000	2100	400
	Rn (Ohms)	500	2850	2000	2100	300
	Vp (Volts)	1800	3000	4000	10,000	2000
	Vn (Volts)	1920	3500	4500	10,500	2500
State 3	t (S)	0.06[a],0.1[b]	0.08[a], 0.12[b]	0.1[a], 0.14[b]	0.16[a]	0.16[a]
$t_0 = 0$[a],	Rp (Ohms)	4500	11,000	7500	7800	10,000
0.12[b],	Rn (Ohms)	4600	11,100	7300	7500	10,100
0.16[a]	Vp (Volts)	10,000	9900	10,200	9200	8900
	Vn (Volts)	10,500	9800	10,000	9800	9100
State 4	t (S)	0.05[a]	0.07[a]	0.083[a]	0.104[a]	0.124[a]
$t_0 = 0$[a]	Rp (Ohms)	200	200	290	165	180
	Rn (Ohms)	220	250	270	185	150
	Vp (Volts)	6550	7500	9100	9100	9500
	Vn (Volts)	6300	7800	9000	9000	8800
State 5	t (S)	0.05[a]	0.08[a]	0.15[a]	0.12[a]	0.14[a]
$t_0 = 0$[a]	Rp (Ohms)	4250	9000	7520	5800	10,000
	Rn (Ohms)	4150	9600	8510	6500	10,500
	Vp (Volts)	8100	7900	9200	9100	8900
	Vn (Volts)	8000	8200	9500	9000	8700

[a] Instant switch is closed.
[b] Instant switch is opened.

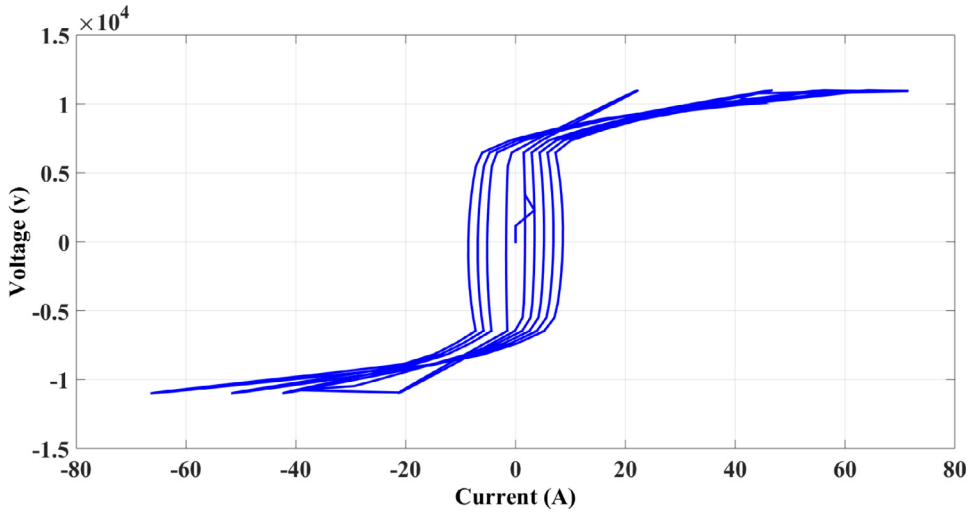

Fig. 4. *V–I* characteristics of state 4.

Besides, the aforementioned equations provide the following three MM filters:

$$\mathrm{MMF1} = (y_d(x) + y_e(x))/2 \tag{5}$$

$$\mathrm{MMF2} = (y_0(x) + y_c(x))/2 \tag{6}$$

$$\mathrm{MMF3} = \{(f(x) \bullet y_0(x)) + (f(x) \circ y_c(x))\}/2 \tag{7}$$

All the above-mentioned MM filters are used to remove noise and keep the features of the original signal. An evaluation of these MM filters conducted on a noisy current signal is presented in Fig. 6. It is observed that MMF3 provides better performance in

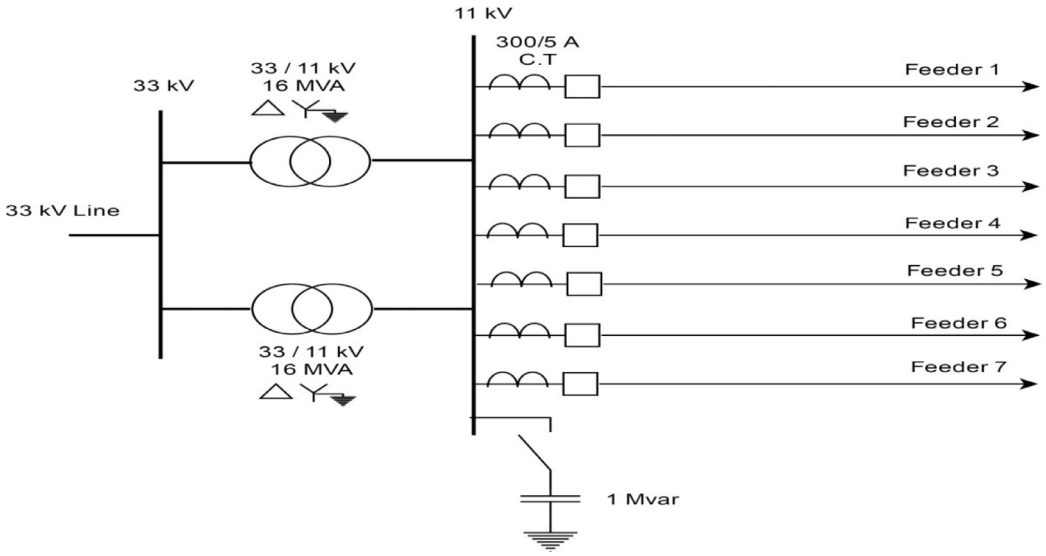

Fig. 5. Electric power distribution system.

Table 2
Electric power distribution system data.

Feeder no.	Load current			Load (MVA)	Length (Km)
	I_a (A)	I_b (A)	I_c (A)		
Feeder 1	56.00	48.00	40.29	0.758	3.6
Feeder 2	146.90	169.80	161.72	3.027	3
Feeder 3	39.00	48.55	30.22	0.570	2
Feeder 4	106.00	97.41	111.34	2.111	1.5
Feeder 5	28.21	26.62	20.04	0.380	4
Feeder 6	69.52	48.42	68.42	1.291	6.8
Feeder 7	15.42	22.94	15.04	0.286	5

Table 3
Test cases.

Event	Simulation conditions	Total
HIF	HIF model resistance varied from 150 Ω to 12 kΩ and DC voltage from 1.5 kV to 10.5 kV randomly to obtain 60 cases. Fault inception angle (0°, 45°, 90°) Source voltage phase angle (0°, 45°, 90°)	540 (60 × 3 × 3)
Load switching	Changes in load level: 0%–25%, 25%–50%, 50%−75%,75%−100% and 100% −110% both forward and reverse conditions. Switching time in a cycle (0°, 45°, 90°) Source voltage phase angle (0°, 45°, 90°)	90 (10 × 3 × 3)
Non-linear load switching	The ratio of linear to non-linear load changes 1 to 0.5 in steps of 0.05 both in forward and reverse conditions. Switching time in a cycle (0°, 45°, 90°) Source voltage phase angle (0°, 45°, 90°)	216 (24 × 3 × 3)
Capacitor Switching	Switching conditions on and off with load variation of 25%, 50%, 75%, 100% and 125%. Switching time in a cycle (0°, 45°, 90°) Source voltage phase angle (0°, 45°, 90°)	90 (5 × 2 × 3 × 3)
Inrush current	No load switching of 33 /11 kV transformer Switching time in a cycle (0°, 30°, 45°, 60°, 90°, 120°,150°, 180°) Source voltage phase angle (0°, 30°, 45°, 60°, 90°, 120°,150°, 180°)	64 (1 × 8 × 8)

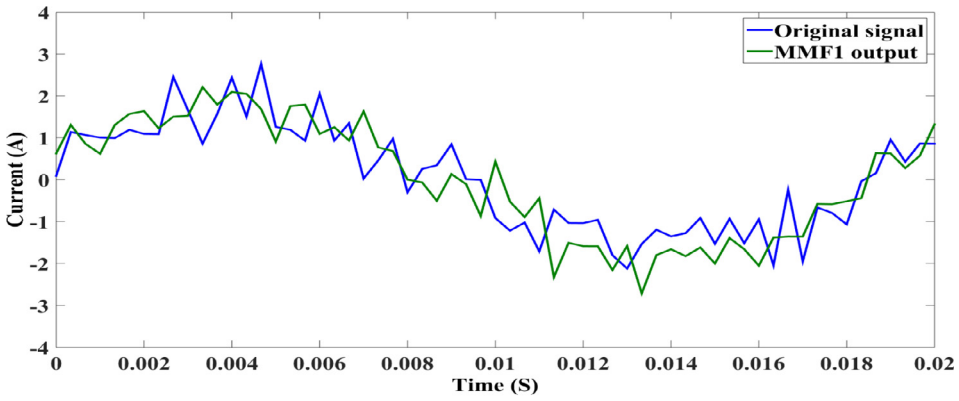

(a)

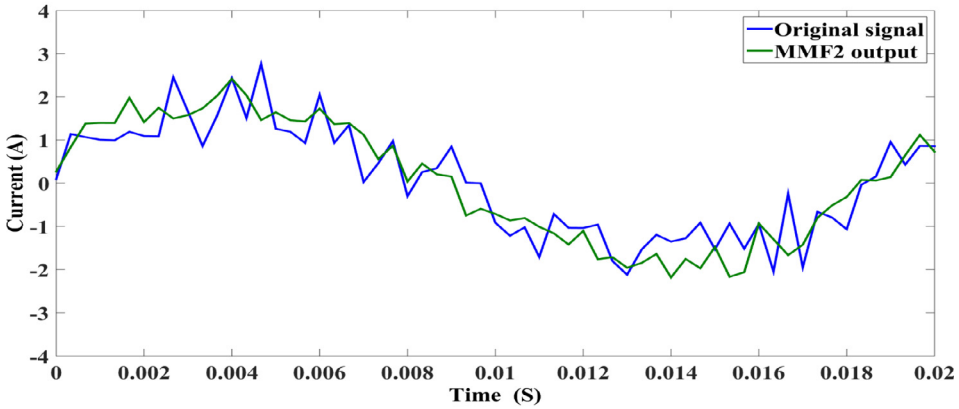

(b)

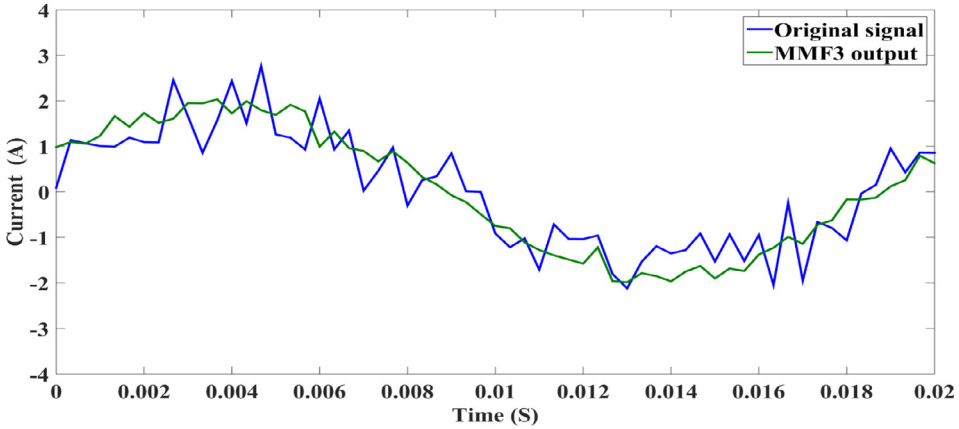

(c)

Fig. 6. Pre-processing performance of the filters (a) MMF1 (b)MMF2 (c) MMF3.

eliminating noise and keeping fault signatures than the other two filters. Thus, MMF3 is used for pre-processing the signal in this work. The length of SE decides the delay in filter output. To reduce the filter delay, flat SE of [0.2 0.8 0.2] is used in this work. The delay of the filter is calculated by the formula given below.

$$\text{Filter delay} = \Delta T \times (y - 1) \tag{8}$$

where ΔT is the sampling interval and y is the length of SE. Thus, the filter delay is 0.66 ms.

6. Feature extraction

The extraction of important and necessary features of the current signal is described below:

1. Mean: It is an average value of the signal.
2. Standard deviation: It is a value that indicates the spread of the signal from the mean.
3. Energy: It is computed using the following equation:

$$\text{Energy} = \frac{1}{T}\int_0^T i^2(t)\,dt \tag{9}$$

where T is the total time period of the signal.

4. Entropy: It is used to determine signal ambiguity and uncertainty. HIF current signal is random in nature. Thus, entropy is used in this work to indicate the uncertainty of energy distribution. Entropy [21] is calculated using the following equation:

$$\text{Entropy} = -\sum p_j \log p_j \tag{10}$$

where p_j is the energy probability distribution of MMF3 output.

5. Kurtosis: It specifies the smoothness of the signal. A bigger kurtosis point represents more outliers in the signal. The formula [22] for computing kurtosis is defined below:

$$\text{Kurtosis} = \left\{\frac{n(n+1)}{(n-1)(n-2)(n-3)}\sum\frac{(x-\bar{x})^4}{\sigma^4}\right\} - \frac{3(n-1)^2}{(n-2)(n-3)} \tag{11}$$

σ- Standard deviation, $\bar{x}$ – Mean, n – number of sample data points.

6. Skewness: It is a measure of the irregularity of the probability distribution of the signal about its mean. It is calculated using the following formula [22]:

$$\text{Skewness} = \left\{\frac{n}{(n-1)(n-2)}\sum\frac{(x-\bar{x})^3}{\sigma^3}\right\} \tag{12}$$

7. Data mining model

Data mining models intend to generate a broad structure that is used to forecast or analyze network performance based on the input data set. Data mining is a tool to create the model and is used for classification [23–25]. Though different data mining classification schemes are available, this study uses two specific data mining models, namely Decision Tree (DT) and Random Forest (RF). The DT is one of the most popular data mining models and it is used in power system engineering applications for classification and decision-making [23,24]. DT is rule-based, more lucid and human-friendly. On the other hand, RF has been chosen due to its superior classification accuracy.

The proposed method utilizes an open source data mining package 'R' for creating the DT model. For HIF detection, DT model has been generated by taking the feature set into account. There are six features which are used to train the DT against the target output of 1 for HIF and 0 for non-HIF.

A total of 1000 cases were simulated out of which 700 cases (70%) were considered for training and 300 cases (30%) for testing. The data mining generated DT model for HIF detection is shown in Fig. 7. It is found that only five (Mean, Skewness, Kurtosis, Standard deviation, and Entropy) of the six features are used for the final decision-making process and are significant in the classification into HIF and non-HIF. Consequently, the following eight rules can be derived from the DT model:

Rule 1: If (mean $<=$ 22.76) & (STD $<=$ 14.764) & (kurtosis $<=$ 3.381), then the status is HIF.
Rule 2: If (mean $<=$ 22.76) & (STD $<=$ 14.764) & (kurtosis $>$ 3.381), then the status is non-HIF.
Rule 3: If (mean $<=$ 22.76) & (STD $>$ 14.764) & (skewness $>=$ −0.2), then the status is HIF.

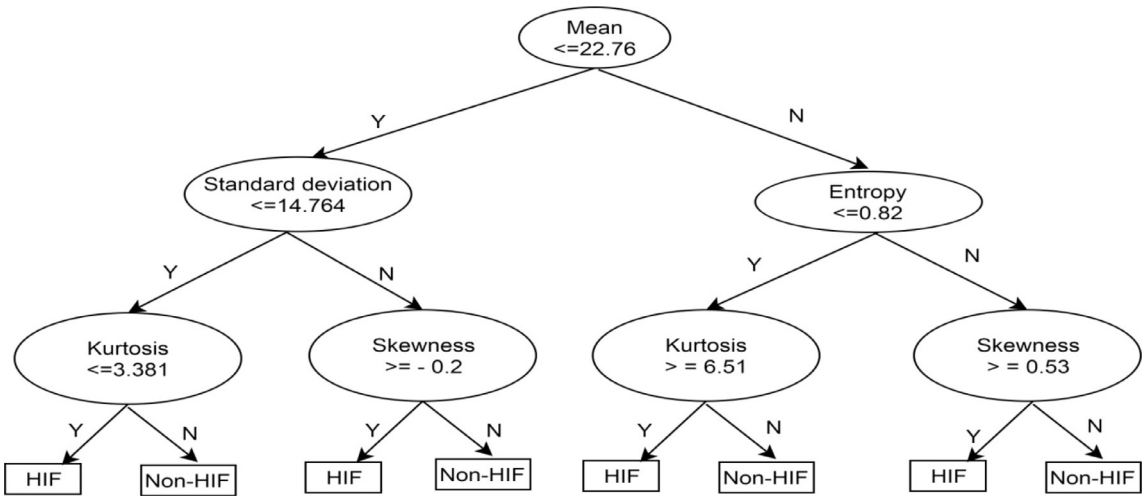

Fig. 7. Decision Tree model.

Rule 4: If (mean $<=$ 22.76) & (STD $>$ 14.764) & (skewness $<$ -0.2), then the status is non-HIF.
Rule 5: If (mean $>$ 22.76) & (entropy $<=$ 0.82) & (kurtosis $>=$ 6.51), then the status is HIF.
Rule 6: If (mean $>$ 22.76) & (entropy $<=$ 0.82) & (kurtosis $<$ 6.51), then the status is non-HIF.
Rule 7: If (mean $>$ 22.76) & (entropy $>$ 0.82) & (skewness $>=$ 0.53), then the status is HIF.
Rule 8: If (mean $>$ 22.76) & (entropy $>$ 0.82) & (skewness $<$ 0.53), then the status is non-HIF.

Testing was performed against 300 cases comprising 162 HIF and 138 non-HIF cases. The confusion matrix of both the data mining models is presented in Table 4. By DT model 160 out of 162 HIF cases were classified correctly and two HIF cases misclassified as non-HIF. On the other hand, in RF method, 161 out of 162 HIF cases were classified correctly, and only one HIF case was misclassified as non-HIF. However, both RF and DT models correctly classify all 138 non-HIF cases.

8. Simulation results

The detection methodology starts with pre-processing of current signal by MM. Then, the features of the current signal are extracted (one, two and three half-cycle data window length) and used as input to the data mining tool to generate the DT model which discriminates between HIF and non-HIF cases. In order to investigate the performance of the proposed method, the complete data set was tested. The following simulation cases are described as examples:

1. *High impedance fault:*

The HIF situation is created in phase A of feeder 6 at fault inception time of 0.1 s by connecting the HIF model as shown in Fig. 1 with arc parameters of the state 1 prescribed in Table 1 about 6 km from the Busbar. The current signal during this HIF condition is given in Fig. 8(a).

2. *Load switching:*

To perform a load switching operation, the load level at phase A of feeder 6 is changed from 75% to 100% (both linear and non-linear switching) at a time $t = 0.1$ s. The current signal observed during this load change is shown in Fig. 8(b).

3. *Capacitance switching:*

Table 4
The confusion matrix.

Predicted	RF		DT	
	1 (HIF)	0 (Non-HIF)	1 (HIF)	0 (Non-HIF)
1 (HIF)	161	0	160	0
0 (Non-HIF)	1	138	2	138

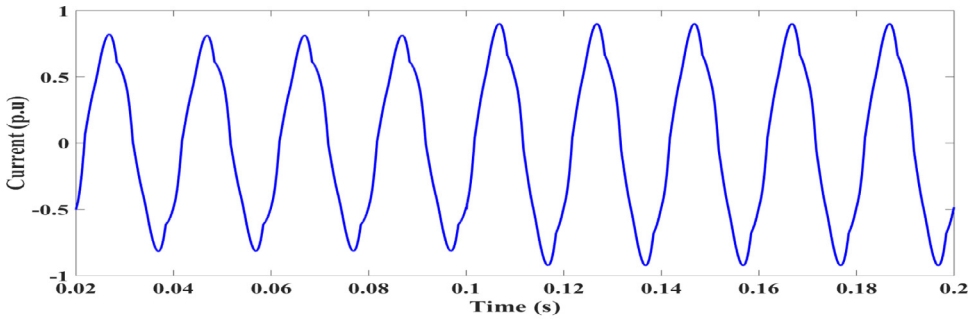

(a)

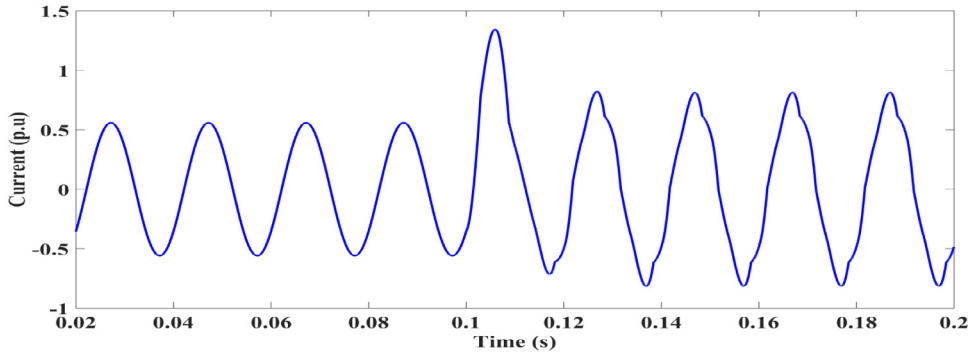

(b)

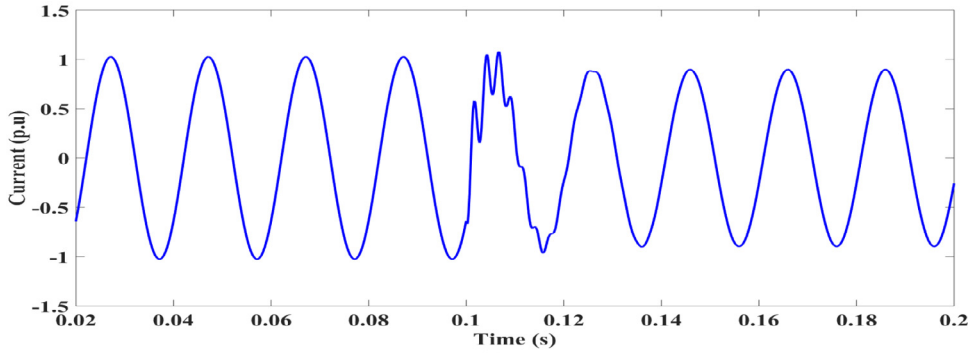

(c)

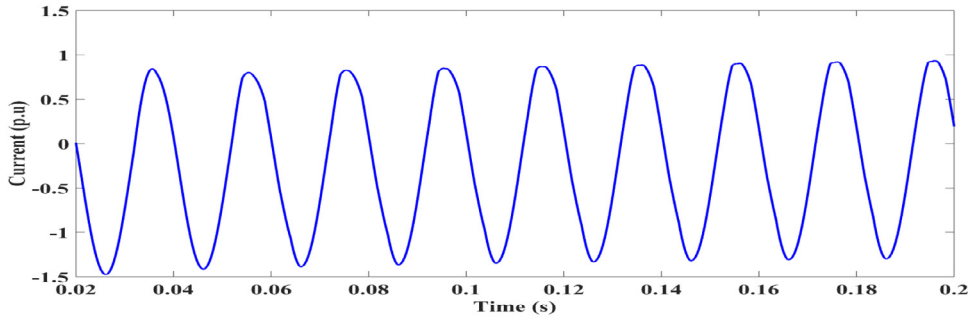

(d)

Fig. 8. Current waveform of (a) HIF (b) Load switching (c) Capacitance switching (d) Transformer inrush.

Table 5
Feature vector of simulated cases.

Features	HIF	Load switching	Capacitance switching	Inrush current
Skewness	−0.0079	0.1246	−0.2402	0.1240
Kurtosis	1.5226	1.821	1.5003	4.813
STD	83.3696	16.249	78.94	0.5616
Mean	0.6045	29.537	0.0362	0.0179
Entropy	1.0364	1.0349	1.0448	4.8449

To perform a capacitance switching operation, the Busbar is connected with a 1 MVAr capacitor bank at a time $t = 0.1$ s and the corresponding current signal is shown in Fig. 8(c).

4. *Inrush current:*

The transformer inrush current was obtained through the simulation of energizing low voltage side of the 33 kV/11 kV transformer, while the primary side was left open, and it is shown in Fig. 8(d).

From the aforementioned conditions, the obtained current signal was treated with MMF3 and the extracted feature (two half-cycle data window length) is presented in Table 5. After applying these data sets to the DT model, it can be concluded that the status of the feeder for the first column feature set is HIF. However, for the rest of the feature sets, feeder status remains normal (non-HIF).

9. Discussions

The proposed HIF detection method was evaluated using the following performance indices:

1. *Dependability:* Total number of HIF conditions predicted/Actual number of HIF conditions considered.
2. *Security:* Total number of non-HIF conditions predicted/Actual number of non-HIF conditions considered.
3. *Accuracy:* Total number of conditions predicted/Actual number of conditions considered.

The performance indices of the DT and RF data mining models were compared as shown in Table 6. It was found that the performance of both the DT and RF data mining model was good except that the dependability of the DT data mining model fell 0.61% below the RF data mining model. Moreover, the complexity of the RF data mining model makes it difficult for real time implementation of the digital signal processor [24]. Hence, the DT data mining model was chosen in this work.

Further, three different data window lengths (one, two and three half-cycles) after the event's inception were used to validate the impact of the data window length. Table 7 shows the performance indices for the three different data window lengths. It was found that there was a significant increase in the performance indices from one half-cycle to two half-cycles. However, the performance indices were almost same in the three half-cycles window length after the inception of HIF. Hence, to reduce the detection time, two half-cycles after event inception was taken as the data window length.

Also, it is well known that power system signals are subject to noise. Hence, it is imperative to analyze the proposed HIF detection scheme under noisy signal input data. Table 8 compares the performance in a noisy atmosphere. It was found that the dependability up to Signal to Noise Ratio (SNR) of 20 dB was similar to the one illustrated in without noise condition. A further increase in SNR decreases the performance indices of the proposed HIF detection scheme. Thus, the proposed HIF detection scheme is appropriate for SNR of less than or equal to 20 dB.

Besides, Table 9 shows a comparison of this work with a previously published paper. There is a considerable improvement shown in the performance of this work except in [6,17]. Although all the HIF cases have been classified correctly, there is a problem of false tripping in [6]. In [17], the total number of test cases considered is as low as 25, which is very less, and there is no evidence of the presence of non-linear load in the system description. Since non-linear load characteristics closely resemble HIF signal, the performance of the detection method in [17] is questionable. Hence, the proposed scheme performs better in all the three performance indices.

Finally, the study was extended to compare detection delay time and it was found that very little research work prescribed a HIF detection delay time [4,13,16,17]. The total detection time of the proposed method is the sum of data window length, filter delay time, and DT processing delay time. Consequently, the time delay for HIF detection in this work is 30.66 ms

Table 6
Comparison of data mining models.

Performance indices	DT	RF
Accuracy	99.34%	99.66%
Security	100%	100%
Dependability	98.77%	99.38%

Table 7
Impact of data window length on the proposed method.

Performance indices	One half- cycle	Two half- cycles	Three half- cycles
Accuracy	98.63%	99.34%	99.34%
Security	98.55%	100%	100%
Dependability	97.53%	98.77%	98.77%

Table 8
Impact of SNR on the proposed method.

Performance indices	15 dB	20 dB	30 dB
Accuracy	99.34%	99.00%	96.66%
Security	100%	99.24%	96.96%
Dependability	98.77%	98.77%	96.29%

Table 9
Comparison of the proposed method with previously published work.

Method	Accuracy	Security	Dependability
Ref [5]	98%	–	–
Ref [6]	93.6%	81.5%	100%
Ref [13]	96%	100%	90%
Ref [16]	97.3%	96.3%	98.3%
Ref [17]	–	100%	100%
The proposed method	99.34%	100%	98.77%

Table 10
Comparison of detection delay.

Method	Detection time
Ref [4]	4 s
Ref [13]	80 ms
Ref [16]	500 ms
Ref [17]	1 s
The Proposed method	30.66 ms

(20 ms + 0.66 ms + 10 ms). Table 10 shows the comparison to the detection delay of previously published work. It is very clear from the table that the proposed method is much faster in HIF detection.

10. Conclusions

A simple and novel technique for high impedance fault detection method has been presented using the current signal with a low sampling rate of 3 KHz. The effectiveness of the proposed detection scheme has been verified on an actual distribution system under different operating conditions and the results show an improved success rate with a detection delay of 30.66 ms.

The proposed method may be improved and extended by considering other comparable signals which could be similar to HIF. Also, the fast-growing distributed generations force to improve the proposed work. So, the future goal of this research is to test the proposed scheme under distributed generations, including other kinds of non-HIF events.

Supplementary materials

Supplementary material associated with this article can be found, in the online version, at doi:10.1016/j.compeleceng.2018.05.010.

References

[1] High impedance fault detection technology, Report of PSRC working group D15. 1996. http://grouper.ieee.org/groups/td/dist/documents/highz.pdf.
[2] Ghaderi A, Mohammadpour HA, Ginn HL. High impedance fault detection – a review. Electr Power Syst Res 2017;143:376–88.
[3] Emanuel A, Cyganski D, Orr J, Shiller S, Gulachenski E. High impedance fault arcing on sandy soil in 15 kV distribution feeders: contributions to the evaluation of the low frequency spectrum. IEEE Trans Power Deliv 1990;5(2):676–86.
[4] Mamishev AV, Russell BD, Benner CL. Analysis of high impedance faults using fractal techniques. IEEE Trans Power Syst 1996;11(1):435–40.

[5] Samantaray SR, Panigrahi BK, Dash PK. High impedance fault detection in power distribution networks using time-frequency transform and probabilistic neural network. IET Gener Trans Distrib 2008;2(2):261–70.
[6] Ghaderi A, Mohammadpour H, Ginn HL, Shin Y. High impedance fault detection in distribution network using time-frequency based algorithm. IEEE Trans Power Deliv 2015;30(3):1260–8.
[7] Bakar AHA, Ali M, Tan C, Mokhlis H, Arof H, Illias H. High impedance fault location in 11 kV underground distribution systems using wavelet transforms. Int J Electr Power Energy Syst 2014;55:723–30.
[8] Santos WC, Lopes FV, Brito NSD, Souza BA. High-impedance fault identification on distribution Networks. IEEE Trans Power Del 2017;32(1):23–32.
[9] Mahari A, Seyed H. High impedance fault protection in transmission lines using a WPT-based algorithm. Int J Electr Power Energy Syst 2015;67:537–45.
[10] Chen J, Phung T, Blackburn T, Ambikairajah E, Zhang D. Detection high impedance fault using current transformer for sensing and identification based method on features extracted using wavelet transform. IET Gener Transm Distrib 2016;10(12):2990–8.
[11] Baqui I, Zamora I, Mazón J, Buigues G. High impedance fault detection methodology using wavelet transform and artificial neural networks. Electr Power Syst Res 2011;81(7):1325–33.
[12] Sedighi AR, Haghifam MR, Malik OP. Soft computing application in high impedance fault detection in distribution system. Electr Power Syst Res 2005;76(1-3):136–44.
[13] Sedighi AR, Haghifam MR, Malik OP, Ghassemian MH. High impedance fault detection based on wavelet transform and statistical pattern recognition. IEEE Trans Power Deliv 2005;20(4):2414–21.
[14] Haghifam MR, Sedighi AR, Malik OP. Development of a fuzzy inference system based on genetic algorithm for high-impedance fault detection. IEE Proc Gener Transm Distrib 2006;153(3):359–67.
[15] Samantaray SR. Ensemble decision trees for high impedance fault detection in power distribution network. Int J Electr Power Energy Syst 2012;43(1):1048–55.
[16] Sarlak M, Shahrtash SM. High impedance fault detection using combination of multilayer perceptron neural networks based on multi resolution morphological gradient features of current waveform. IET Gener Transm Distrib 2011;5(5):588–95.
[17] Gautam S, Brahma SM. Detection of High impedance fault in power distribution systems using mathematical morphology. IEEE Trans Power Sys 2013;28(2):1226–34.
[18] Sedighi AR. A new model for high impedance fault in electrical distribution system. Int J Sci Res Comput Sci Eng 2014;2(4):6–12.
[19] Gautam S, Brahma SM. Guidelines for selection of an optimal structuring element for mathematical morphology based tools to detect power system disturbances. Proceedings of IEEE power & energy society general meeting. 2012. p. 1–6.
[20] Gautam S, Brahma SM. Properties of mathematical morphology based filter for online filtering of power system signals. Proceedings of IEEE 41st North American power symp. 2009. p. 1–5.
[21] Chandrashekar G, Sahin F. A survey on feature selection methods. Comput Electr Eng 2014;40(1):16–28.
[22] Sugumaran V, Ramachandran KI. Automatic rule learning using decision tree for fuzzy classifier in fault diagnosis of roller bearing. Mech Syst Signal Process 2007;21(5):2237–47.
[23] Kar S, Samantaray SR, Zadeh MD. Data mining model based intelligent differential micro grid protection scheme. IEEE Syst J 2017;11(2):1161–9.
[24] Mishra DP, Samantaray SR, Joos G. A combined wavelet and data-mining based intelligent protection scheme for microgrid. IEEE Trans Smart Grid 2016;7(5):2295–304.
[25] Han J, Kamber M, Pei J. Data mining: concepts and techniques. Elsevier; 2011.

Kavaskar Sekar received his M.E. degree in Power Systems Engineering from Anna University, Tamil Nadu, India. Currently, doing Research at Anna University in the Department of Electrical and Electronics Engineering. His research areas are Power system protection and power system disturbances.

Nalin Kant Mohanty received his M.Tech degree in Computer Applications in Industrial Drives from Visveswaraiah Technological University, Karnataka and Ph.D. degree from Anna University, Tamil Nadu, India. Currently, he is working as Professor in the Department of Electrical and Electronics Engineering, Sri Venkateswara College of Engineering, Tamil Nadu, India. His research areas are Power Electronics drives and control, and Power system protection.